

## Magnetic Excitations in the $S = 1/2$ Alternating Chain Compound $(\text{VO})_2\text{P}_2\text{O}_7$

A. W. Garrett,<sup>1</sup> S. E. Nagler,<sup>2</sup> D. A. Tennant,<sup>2</sup> B. C. Sales,<sup>2</sup> and T. Barnes<sup>2,3</sup>

<sup>1</sup>Department of Physics, University of Florida, Gainesville, Florida 32611-0448

<sup>2</sup>Oak Ridge National Laboratory, Oak Ridge, Tennessee 37831-6393

<sup>3</sup>Department of Physics and Astronomy, University of Tennessee, Knoxville, Tennessee 37996-1501

(Received 9 April 1997)

Magnetic excitations in an array of  $(\text{VO})_2\text{P}_2\text{O}_7$  single crystals have been measured using inelastic neutron scattering. Until now,  $(\text{VO})_2\text{P}_2\text{O}_7$  has been thought of as a two-leg antiferromagnetic Heisenberg spin ladder with chains running in the  $a$  direction. The present results show unequivocally that  $(\text{VO})_2\text{P}_2\text{O}_7$  is best described as an alternating spin chain directed along the crystallographic  $b$  direction. In addition to the expected magnon with magnetic zone-center energy gap  $\Delta = 3.1$  meV, a second excitation is observed at an energy just below  $2\Delta$ . The higher mode may be a triplet two-magnon bound state. [S0031-9007(97)03725-3]

PACS numbers: 75.10.Jm, 75.10.Hk, 75.30.Ds

Spin gaps are found in many low dimensional interacting quantum spin systems. Some examples include integer-spin Heisenberg antiferromagnetic chains [1], spin-Peierls systems [2], and spin ladders [3,4]. There has been particular recent interest in spin ladders arising from the novel prediction that gaps should be present only in even-leg ladders and the possibility that doped ladders may exhibit superconductivity [3]. The insulating magnetic salt  $(\text{VO})_2\text{P}_2\text{O}_7$  (VOPO) has been widely considered to be an excellent realization of the two-leg antiferromagnetic Heisenberg spin ladder [5]. In this Letter we report results from inelastic neutron scattering experiments using an aligned array of VOPO single crystals. Our results show conclusively that the magnetic properties of VOPO are not those of a spin ladder. VOPO is instead found to be an alternating Heisenberg antiferromagnetic chain, with weak ferromagnetic interchain couplings. Moreover, the magnetic chains in VOPO run perpendicular to the supposed ladder direction. The measured alternation parameter describing VOPO is in the interesting regime in which a novel two-magnon bound state may occur [6].

The crystal structure of VOPO is nearly orthorhombic, with a slight monoclinic distortion so that the space group is  $P2_1$  [7]. The room temperature lattice parameters are  $a = 7.73$  Å,  $b = 16.59$  Å,  $c = 9.58$  Å, and  $\beta = 89.98^\circ$ . The magnetic properties of VOPO arise from  $S = 1/2$   $\text{V}^{4+}$  ions situated within distorted  $\text{VO}_6$  octahedra. Face-sharing pairs of  $\text{VO}_6$  octahedra are stacked in two-leg ladder structures oriented along the  $a$  axis. The ladders are separated by large, covalently bonded  $\text{PO}_4$  complexes. The V-V nearest neighbor distance in the  $a$  direction is approximately 3.86 Å, one half of a lattice spacing. Along the  $b$  ("rung") direction the mean V-V distance is 3.2 Å within the ladder. The interladder V-V distance across the  $\text{PO}_4$  groups is 5.1 Å. The structure is illustrated schematically in Fig. 1.

The susceptibility of VOPO powder was investigated by Johnston *et al.* [5]. Although the susceptibility could be

accurately reproduced by either a spin ladder (with  $J_{\parallel} \approx J_{\perp}$ ) or by an alternating chain [5,8], the expectation that the  $\text{PO}_4$  group would provide a weak superexchange path led to a preference for the spin ladder interpretation of VOPO. The proposed spin ladder is illustrated schematically in Fig. 1. Motivated by the detailed theoretical predictions for the excitation spectrum of a spin ladder [8], Eccleston *et al.* [9] used pulsed inelastic neutron scattering to probe the dynamic magnetic properties of VOPO powders. Their measurement of a spin gap of 3.7 meV was interpreted as further support for the ladder model.

The surprising discovery of a second spin excitation near 6 meV in a recent triple-axis neutron scattering experiment [10] on VOPO powder is inconsistent with a simple spin ladder model. It has long been known that measurements of static magnetic properties cannot easily distinguish between spin ladder and alternating chain

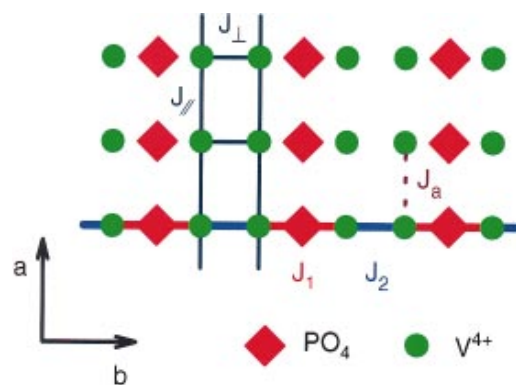


FIG. 1(color). Schematic depiction of the structure and magnetic interactions in VOPO. The spin ladder model previously thought to describe VOPO has nearest neighbor exchange constants  $J_{\parallel}$  along the  $a$  (ladder) direction and  $J_{\perp}$  along the  $b$  (rung) direction. In the alternating chain model, nearest neighbor  $\text{V}^{4+}$  ions are alternately coupled by constants  $J_1$  and  $J_2$  along the  $b$  (chain) direction. Neighboring spins in adjacent chains are coupled by  $J_a$ . Magnetic coupling in the  $c$  direction is negligible.

models [11], and also that measurements on powders can be difficult to interpret. For these reasons we undertook studies of spin dynamics in VOPO single crystals.

Single crystals of  $(\text{VO})_2\text{P}_2\text{O}_7$  were grown using a method described previously [10]. To achieve sufficient sample volume for inelastic neutron scattering measurements, approximately 200 single crystals of typical size  $1 \times 1 \times 0.25 \text{ mm}^3$  were aligned, mounted on thin aluminum plates, and assembled into an array. The resulting sample had an approximate total mass of 1 g and an effective mosaic spread of  $8^\circ$ – $10^\circ$  FWHM. Although not optimal, this proved to be adequate for the present purpose.

Inelastic neutron scattering measurements were carried out using the HB1, HB1A, and HB3 triple-axis spectrometers at the HFIR reactor, Oak Ridge National Laboratory. Several different instrumental configurations were utilized, including fixed incident or fixed final energies of 14.7, 13.5, or 30.5 meV. For temperature control the VOPO array was mounted either in a closed cycle refrigerator or in a flow cryostat. Both  $(h, k, 0)$  and  $(0, k, l)$  scattering planes were used in different experiments.

Typical constant- $\vec{Q}$  scans are illustrated in Fig. 2. The left panels show measurements at  $(1, -2, 0)$  at temperatures of 10 K (lower panel) and 30 K (upper panel). The 10 K scan clearly shows two peaks, and the reduced intensity at the higher temperature is indicative of

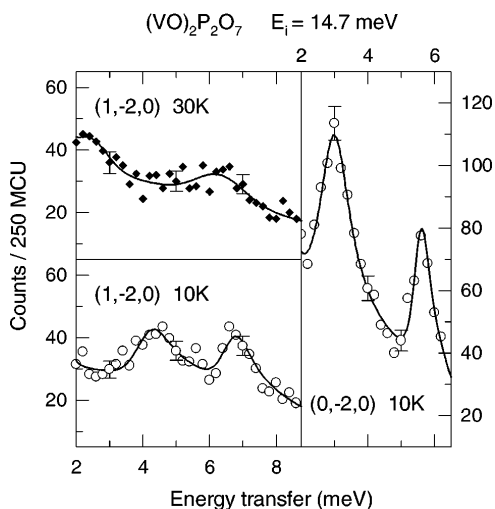


FIG. 2. Typical constant- $\vec{Q}$  scans at  $\vec{Q} = (1, -2, 0)$  (left panels) and  $\vec{Q} = (0, -2, 0)$  (right panel). The scans shown were taken at the HB1A spectrometer with fixed incident neutron energy of 14.7 meV and collimations  $40' - 40' - 40' - 68'$ . The energy resolution at zero energy transfer is  $0.91(2) \text{ meV}$  FWHM. The solid lines running through the 10 K data are least-squares fits of a convolution of the instrumental resolution with delta function excitations obeying the dispersion relations of Eq. (2). The solid line through the 30 K data is a guide to the eye. Intensities are normalized to a fixed number of incident neutrons expressed by monitor count units (MCU). Some representative  $1\sigma$  error bars are shown.

their magnetic origin. The right panel shows a 10 K scan at  $\vec{Q} = (0, -2, 0)$ , where the peaks are slightly lower in energy and are much more intense than at  $(1, -2, 0)$ . The temperature and  $Q$  dependence of the scattering was used to verify the magnetic nature of the peaks for several wave vectors, including zone centers and zone boundaries in all three directions.

The solid lines through the 10 K data are obtained by a least-squares fit of the data to a convolution of the full instrumental resolution with delta function excitations using dispersion relations discussed below. The nonmagnetic background used in the fit consists of a Gaussian peak centered at zero energy accounting for incoherent and (at some wave vectors) Bragg scattering, plus a linearly sloping background. At low temperatures the peak widths are resolution limited. The significant intensity difference between  $(1, -2, 0)$  and  $(0, -2, 0)$  is seen to be a consequence of resolution combined with the large mosaic spread of the sample. Simple Gaussian fits to obtain the peak positions gave the same results as full convolutions. The peak positions were determined at various wave vectors.

Figure 3 shows the measured dispersion along the crystal axis directions indicated. Several features are immediately apparent. The combination of steep dispersion, large sample mosaic, and two modes gives broadened error bars midway across the zone in the  $(0, \zeta, 0)$  direction. The excitation energies have at most a very weak dependence on the  $Q_c$  component of the wave vector (middle panel). The dependence of energy on  $Q_a$  (in the “ladder” direction) is much weaker than on  $Q_b$  (in the rung direction). This

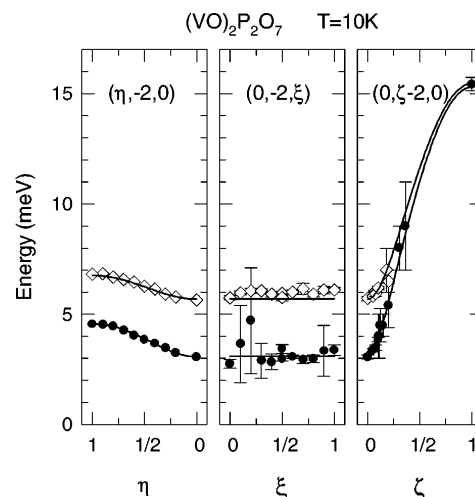


FIG. 3. Measured dispersion of magnetic excitations in VOPO at  $T = 10 \text{ K}$ . When not visible error bars are smaller than the size of the plotted symbols. Filled circles (open diamonds) are points from the lower (upper) energy mode. The solid lines are dispersion curves calculated using parameters obtained by fitting Eq. (2) to the observed peak positions. Wave vectors are plotted in units corresponding to the VOPO reciprocal lattice.

implies that the magnetic coupling which supports spin waves is indeed dominantly one dimensional, but that the strongest coupling is along the  $b$  direction. Moreover, the dispersion shows that the exchange in the ladder direction is *ferromagnetic* in nature.

The observed spectrum of magnetic excitations in VOPO is clearly inconsistent with a two-leg spin ladder. A better model must account for the strong dispersion in the  $b$  direction, the presence of a spin gap, and be compatible with the crystal structure of VOPO. The most likely model is that of weakly coupled antiferromagnetic alternating chains running in the  $b$  direction. The gap is a consequence of the spin dimerization inherent in the VOPO crystal structure.

A correct theory for VOPO must also explain the presence of two magnetic modes. Since the high temperature limit of the magnetic susceptibility [5] is exactly that expected for  $S = 1/2$ ,  $g = 2$ , the possibility that the upper mode is a low lying single ion excitation can be ruled out.

One potential explanation for a second mode is splitting of a triplet magnon level by anisotropy. Using the three inequivalent exchanges  $J_1$ ,  $J_2$ , and  $J_a$  shown in Fig. 1 the Hamiltonian can be written

$$\hat{H} = \sum_{l,m} \sum_{\alpha=x,y,z} \{ J_a^{\alpha\alpha} S_{l,m}^{\alpha} S_{l+1,m}^{\alpha} + J_1^{\alpha\alpha} S_{l,2m-1}^{\alpha} S_{l,2m}^{\alpha} + J_2^{\alpha\alpha} S_{l,2m}^{\alpha} S_{l,2m+1}^{\alpha} \}, \quad (1)$$

where the index  $l(m)$  runs over spin sites in the  $\vec{a}(\vec{b})$  direction. The anisotropic exchange is represented by diagonal matrices  $J_{\nu}^{\alpha\alpha} = J_{\nu}[\delta^{\alpha z} + \epsilon_{\nu}(\delta^{\alpha x} + \delta^{\alpha y})]$  for  $\nu = 1, 2, a$ . Here  $z$  is an arbitrarily chosen unique axial direction for exchange anisotropy.

The excitation energies can be calculated using a pseudoboson technique appropriate for dimerized chains [12]. To first order this agrees with perturbation theory from the isolated dimer limit [13]. In this approximation the anisotropy leads to an  $S^z = 0$  longitudinal (L) mode and a doubly degenerate  $S^z = \pm 1$  transverse (T) mode,

$$\omega_{\vec{Q}}^L = \{\epsilon_1 J_1 [\epsilon_1 J_1 - J_2 \cos(\pi Q_b) + 2J_a \cos(\pi Q_a)]\}^{1/2},$$

$$\omega_{\vec{Q}}^T = \{J_1(1 + \epsilon_1)/2 [J_1(1 + \epsilon_1)/2 - \epsilon_2 J_2 \cos(\pi Q_b) + 2\epsilon_a J_a \cos(\pi Q_a)]\}^{1/2}. \quad (2)$$

The solid lines in Fig. 3 are the result of a least-squares fit of Eq. (2) to the data. Two equally good descriptions of the data are possible depending on whether the upper mode (A) or lower mode (B) is chosen as the longitudinal branch; the results are summarized in Table I.

In principle, the  $\vec{Q}$  dependence of the mode intensity should allow one to distinguish between the L and T modes if the model is applicable. In the present experiment this is complicated by the large effective sample mosaic which dominates the observed changes in mode intensity as the direction of  $\vec{Q}$  is varied. Nevertheless, it can be stated that both modes appear with similar intensities for all directions measured. This is unexpected in the anisotropic exchange model.

TABLE I. Anisotropic exchange parameters.

Parameter	Fit A	Fit B
$J_a$ (meV)	-0.27(2)	-0.24(2)
$\epsilon_a$	0.91(7)	1.13(9)
$J_1$ (meV)	10.30(14)	12.32(55)
$\epsilon_1$	1.16(3)	0.93(5)
$J_2$ (meV)	8.7(3)	10.18(15)
$\epsilon_2$	1.12(2)	0.85(4)

Fits to the observed dispersion require strong V-V exchange through the  $\text{PO}_4$  groups. A similarly strong exchange mediated by a  $\text{PO}_4$  complex has recently been found in the chemical precursor compound of VOPO,  $\text{VODPO}_4 \cdot \frac{1}{2} \text{D}_2\text{O}$  [14], which contains magnetically isolated  $S = 1/2$  V-V dimers. Relatively strong superexchange through the  $\text{PO}_4$  groups is possible because of coherent molecular electron orbitals in the complex. Beltrán-Porter *et al.* [15] anticipated the importance of superexchange through  $\text{PO}_4$  in VOPO and proposed an alternating chain in the  $b$  direction, which is in agreement with the present result.

Although Eq. (2) gives an excellent account of the data, considerable exchange anisotropy is necessary to account for the mode splitting. Recent single crystal magnetic susceptibility measurements [16] were quantitatively consistent with the previous powder results [5] and found little, if any, evidence for anisotropy. Further, the exchange coupling in the precursor compound  $\text{VODPO}_4 \cdot \frac{1}{2} \text{D}_2\text{O}$  was found to be isotropic [14]. These facts suggest that one should seek another explanation for the second mode.

In a recent paper [6], Uhrig and Schulz have considered the excitations of an alternating  $S = 1/2$  Heisenberg chain with isotropic exchange [Eq. (1) with  $\epsilon_1 = \epsilon_2 = 1$  and  $J_a = 0$ ] in the continuum limit using field theoretical methods. The basic excitations are triplet magnons with an energy gap  $\Delta$ . The magnitude of  $\Delta$  depends on the alternation parameter  $\delta = (\beta - 1)/(\beta + 1)$  where  $\beta = J_1/J_2$ . The limit  $\delta = 0$  corresponds to the usual antiferromagnetic Heisenberg chain for which the excitations are free spinons resulting in the well known continuum excitation spectrum [17]. For  $\delta > 0$  a gap opens in the spectrum [6,18] and the lowest lying magnetic excitation is a well defined  $S = 1$  triplet mode. For small  $\delta$  one expects a second gap to the remnant of the original continuum at an energy of  $2\Delta$ . Both the continuum [19] and second gap [20] have been reported in  $\text{CuGeO}_3$ , for which  $\delta \leq 0.05$ . The theory further predicts that for  $\delta \geq 0.082$  a second sharp triplet mode appears at energies just below the continuum [6]. This mode is a two-magnon bound state. Assuming isotropic exchange the alternation parameter describing VOPO is  $\delta \approx 0.1$ , in the regime where this mode should be visible. Given the evidence in favor of isotropic exchange in VOPO, it is plausible that the observed second mode is, in fact, the two-magnon bound state.

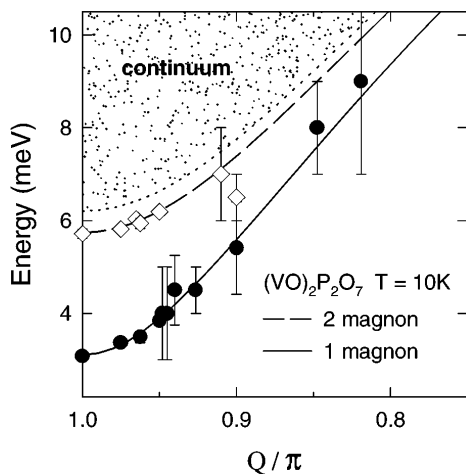


FIG. 4. Closeup of the measured dispersion in VOPO in the chain direction near the antiferromagnetic zone center  $(0, -2, 0)$ , ( $Q = \pi$  in reduced units). The lines through the upper and lower modes are from a fit of Eq. (3) to the data for wave vectors along the chain direction alone. The hypothesized continuum is illustrated schematically.

Figure 4 shows an expanded view of the dispersion in VOPO along the chain direction near  $\vec{Q} = (0, -2, 0)$ , which corresponds to  $Q = \pi$  in reduced units. The solid and dashed lines are the result of fitting the one-dimensional lower ( $l$ ) and upper ( $u$ ) mode dispersions to the expression

$$\omega_Q^{l,u} = \sqrt{\left(\frac{\pi}{2} J\right)^2 \sin^2(Q) + \Delta_{l,u}^2}, \quad (3)$$

resulting in  $J = 9.3(1)$  meV,  $\Delta_l = 3.12(3)$  meV, and  $\Delta_u = 5.75(2)$  meV. The expression for the lower mode in Eq. (3) agrees with the predictions of the continuum model [6] for  $Q \approx \pi$ . The value of  $\Delta_l/J$  allows a determination of  $\delta$  using the results of numerical computations [6]. Note that  $J = (J_1 + J_2)/2$ . The value of  $\Delta_u$  is slightly less than  $2\Delta_l$  as expected for the two-magnon bound state. In contrast, if the second mode is a consequence of anisotropy this proximity is purely accidental. We believe that a two-magnon bound state is the best explanation for the upper magnetic mode.

Several open questions about this interpretation remain. The substantial intensity of the upper mode is very unusual for two-magnon scattering. As indicated schematically in Fig. 4 there may also be a higher lying continuum of excitations but no clear sign of this has appeared in our measurements to date. Detailed theoretical calculations of

the expected neutron scattering response would be of great interest. Light scattering measurements may be sensitive to two-magnon states and should also be instructive.

In the presence of a sufficiently strong external magnetic field the predicted mode splittings of the two proposed models are very different. Unfortunately such experiments are extremely difficult with the VOPO samples available to date. A suitably large *single* crystal is necessary for this as well as for careful investigations of the mode intensities as a function of  $Q$  and  $T$ . Continuing efforts are underway to obtain the desired sample.

We would like to acknowledge useful interactions with P. Dai, J. Fernandez-Baca, H. Mook, and J. Zarestky. We thank J. Thompson for sharing results of susceptibility measurements with us prior to publication. Expert technical assistance was provided by S. Moore and B. Taylor. This work was supported in part by the United States Department of Energy under Contract No. DE-FG05-96ER45280 at the University of Florida, and by Oak Ridge National Laboratory, managed for the U.S. D.O.E. by Lockheed Martin Energy Research Corporation under Contract No. DE-AC05-96OR22464.

- [1] F. D. M. Haldane, Phys. Rev. Lett. **50**, 1153 (1983).
- [2] M. Nishi *et al.*, Phys. Rev. B **50**, 6508 (1994).
- [3] For a recent review of spin ladders see E. Dagotto and T. M. Rice, Science **271**, 618 (1996). See also Phys. Today **49**, No. 10, 17 (1996).
- [4] S. A. Carter *et al.*, Phys. Rev. Lett. **77**, 1378 (1996).
- [5] D. C. Johnston *et al.*, Phys. Rev. B **35**, 219 (1987).
- [6] G. S. Uhrig and H. J. Schulz, Phys. Rev. B **54**, R9624 (1996).
- [7] P. T. Nguyen *et al.*, Mater. Res. Bull. **30**, 1055 (1995).
- [8] T. Barnes and J. Riera, Phys. Rev. B **50**, 6817 (1994).
- [9] R. S. Eccleston *et al.*, Phys. Rev. Lett. **73**, 2626 (1994).
- [10] A. W. Garrett *et al.*, Phys. Rev. B **55**, 3631 (1997).
- [11] J. Eckert *et al.*, Phys. Rev. B **20**, 4596 (1979).
- [12] R. A. Cowley *et al.*, J. Phys. Condens. Matter **8**, L179 (1996).
- [13] A. B. Harris, Phys. Rev. B **7**, 3166 (1973).
- [14] D. A. Tennant *et al.*, Phys. Rev. Lett. (to be published).
- [15] D. Beltrán-Porter *et al.*, Solid State Ion. **32-33**, 57 (1989).
- [16] J. R. Thompson and K. J. Song (private communication).
- [17] D. A. Tennant *et al.*, Phys. Rev. Lett. **70**, 4003 (1993).
- [18] A. M. Tsvelik, Phys. Rev. B **45**, 486 (1992).
- [19] M. Arai *et al.*, Phys. Rev. Lett. **77**, 3649 (1996).
- [20] M. Aïin *et al.*, Phys. Rev. Lett. **78**, 1560 (1997).